NUMERICAL STUDIES OF FLOWS THROUGH MICRO- AND NANO-CHANNELS WITH DIFFERENT BOUNDARY CONDITIONS

M. S. Ozhgibesov[1], T. S. Leu[1], C. H. Cheng[1], A. V. Utkin[2], V. M. Fomin[2], I. F. Golovnev[2]

[1]Department of Aeronautics and Astronautics, National Cheng Kung University
Tainan 701, Taiwan R.O.C.,
[2]Khristianovich Institute of Theoretical and Applied Mechanics SB RAS
Novosibirsk, 630090, Russia

Introduction

Improvements in microfabrication as well as falling prices due to this progress have grown the application area of microsystems, so that has motivated many engineers and researchers dealing with microchannels which are significant parts of many micro-electro-mechanical-systems (MEMS). They have many ways of applications. Biochemical reaction chambers, heat exchanger and physical particle separators are also the possible applications. In order to study the microflow behaviors in these devices, one can refer to results of theoretical and experimental investigations available in the literature.

One of the earliest experimental study of gas flow through copper membrane has been conducted by Warrick and Mack [1]. Hanks and Weissberg [2] have proposed and semiempirical equation for the pressure driven flow through a circular channel. This relation was recently tested by Shinagawa et al. [3] and it was found to be valid in the range of the continuum to the upper limit of transition regimes. There are a lot of studies of both temperature and pressure driven flows through long channels, for example works by Sharipov et al. [4, 6] and Shen et al. [5]. On the other hand the gas flows through extremely short channels (slits and orifices) have been intensively studied as well, see for example work of Lilly et al. [7] or report by Fujimoto and Usami [8]. Sreekanth [9] has conducted experimental studies of rarefied gas flow through short channels in a wide range of pressure ratios. This paper proposes a semiempirical equation for estimation of mass flow rate:

$$\dot{m} = \left[\frac{\pi {d_{ch}}^4}{128 \mu R T_1} \frac{P_1 + P_2}{2} \Delta P + \frac{0.519 {d_{ch}}^3}{\langle V_1 \rangle} \right] \frac{1}{L_{ch}\left(1 + d_{ch}/L_{ch}\right)}, \qquad (1)$$

where $<V>$ is the average molecular velocity; μ – viscosity of the gas; P and T are the pressure and temperature of the gas, respectively. Variables with subscripts 1 and 2 correspond to the parameters of gas in the upstream and downstream reservoirs. This relation was obtained for the case of transition flow through the extremely short tubes ($L_{ch}/d_{ch}<1$ - length to diameter ratio).

The applications of membranes to gas separations have been recently reviewed by Bernado et al. [10]. Commonly numerical or analytical investigations of gas flows through the membrane are performed considering one separated channel or a small set of parallel channels with further extrapolation of the results to the case of membrane using correction factors [11]. Unfortunately the real membranes may have highly curved or intersecting channels and analysis of gas flow through such systems is a sophisticated issue. The way to solve this problem is to approximate the long curved/branched channel by set of short channels ($L_{ch}/d_{ch}\approx1$) connected to each other. One of the problems arising on the way is that most of works describe gas flows through the long straight channel or through the extremely short one while middle-size channels are almost undiscussed. Another problem is most of the theoretical studies on rarefied gas flow were performed with assumption of diffusive interactions between gas atoms and channel's surfaces, this approach might by valid in case if the walls of the channels have imperfections (contaminations, scratches and etc.). On the other hand, precision of MEMS manufacturing growth day to day. Results described in [14]

show that diffusive model is not able to reproduce all the processes accompanying collisions of gas atoms with clean metal surface.

The aim of this study is to proceed the numerical simulation of argon flow through long and middle-size channels in order to define the region of applicability of relations derived in [12, 13] for the case of long channel, but without specifying the term “long”. We have considered three different types of boundary conditions (BC): specular interactions; diffusive model (this model of BC was commonly used in papers mentioned above) and the channel with atomic structure corresponding to the structure of tungsten. All investigations described in present work have been performed using Molecular Dynamics (MD) simulation method. We have observed that the choice of BC influences on the flow properties and the significance grows with respect to the channel’s length. Another important impact of this paper is the defined region of validity of relations shown in [12, 13] for predictions of mass flow rate.

Methodology

The studied model is presented in Figure 1. This 3D system consists of two rectangular tanks filled with argon with values of pressure and temperature of P_1, T_1 and P_2, T_2, respectively. The argon flows between tanks through the channel of square cross-section attached to the tank’s wall.

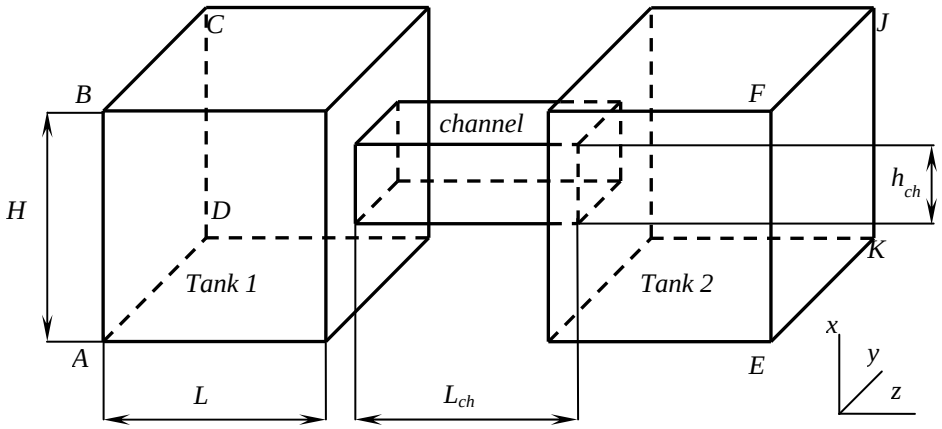

Figure 1. Sketch of the system used for simulations.
H and L – height and length of the tanks; H_{ch} and L_{ch} – height and length of the channel;

It was found that the lateral dimensions of the tank must be at least 8 times greater that the corresponding sizes of the channel ($H/h_{ch} \geq 8$); it guarantees that flow properties are not affected by the boundaries of the vessel. The pressure in the vessels was maintained at the constant value by adding new gas atoms to the left quarter of the tank, in case of the left tank, and to the right quarter – in case of the right one. Specular boundary conditions (BC) are set up on the 7 faces of the tank, while the leftmost and the rightmost faces (ABCD and EFJK) are free of a boundary, i.e. gas atoms are allowed to migrate through them. Atoms that passed through the plane ABCD or EFJK were excluded from the simulation. The total flow rate was estimated as follows:

$$J_{12} = \frac{\Delta N_{12} - \Delta N_{21}}{t}, \qquad (2)$$

where ΔN_{12} and ΔN_{21} - the number of argon atoms have passed from the first vessel into the second one and vice versa, respectively; t - the time elapsed from the start of the simulation.

It should be noted that the positive value of J_{12} corresponds to the case when the flow from the left the tank exceeds the flow from the right one.

The results obtained for this flow configuration are discussed in terms of three parameters: the length-to-height ration of the channel; the pressure ratio P_2/P_1, and the rarefaction parameter [6]:

$$\delta = \frac{\sqrt{\pi}}{2}\frac{h_{ch}}{\lambda} = \frac{\sqrt{\pi}}{2}\frac{1}{\mathrm{Kn}} \tag{3}$$

where λ is the molecular mean free path; h_{ch} is the height of the channel. Once can see that the rarefaction parameter is inversely proportional to the Knudsen number, hence the limit $\delta = 0$ represents the free-molecular regime, while $\delta \to \infty$ corresponds to the continuum mechanics regime.

The reduced flow rate W through the channel is defined as:

$$W = \frac{J_{12}}{J_1}, \tag{4}$$

where J_{12} is the flow rate through the channel at any L_{ch}/h_{ch} , P_2/P_1 and δ, while:

$$J_1 = \frac{n_1 \langle V_1 \rangle}{4} {h_{ch}}^2, \tag{5}$$

is the flow rate through a square orifice (L_{ch}/h_{ch}=0) into vacuum (P_2/P_1=0) at the free molecular limit and it is calculated analytically. $<V_1>$ is the average molecular speed at given temperature T_1 and n_1 is the gas concentration.

We have considered three types of BC on the inner surfaces of the channel:

- Specular reflection;
- Maxwell model, it is also called diffusive BC;
- "Real channel", i.e. the channel with walls represented by a set of tungsten atoms.

Implementations of the first two BC are straightforward and discussed in many studies, for example [15]. The third channel was created by the removal of excess atoms of the tungsten bar (atoms of the bar are arranged according with BCC structure of tungsten). This process is illustrated in Figure 2,*a*.

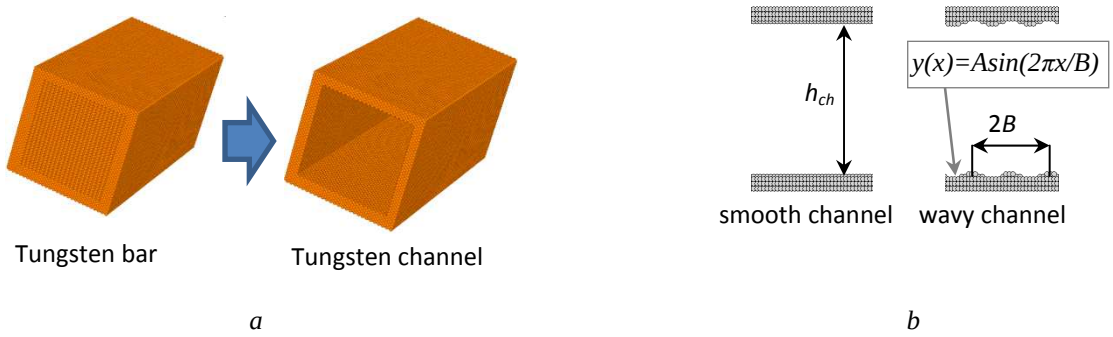

a *b*

Figure 2. Sketch of tungsten channel used for simulations (*a*); side view of the channel with smooth and wavy walls (*b*).

B – is the wavelength; h_{ch} – height of the channel.

Walls of the channel consist of six atomic layers and atoms that comprised the outer layers were held fixed in their equilibrium lattice positions, while the atoms in other two layers were permitted to move according to the appropriate classical equations of motion. In order to demonstrate the influence of the channel's irregularities on the flow we have considered two kinds of real channel: with smooth and wavy walls, see left and right picture, respectively, on the Figure 2,*b*.

Initial velocities of the tungsten atoms were determined from the Maxwell distribution function corresponding to the desired temperature of the channel T_{ch}. The simple velocity scaling method has been used to maintain the temperature of the tungsten at constant value.

The interactions among tungsten atoms were taken as being sums of pairwise Morse potential:

$$\Phi_{W-W} = \begin{cases} D_W \left[e^{-2B_W(r-R_W)} - 2e^{-B_W(r-R_W)} \right], 0 < r < 2.3R_W \\ 0, r \geq 2.3R_W \end{cases}, \quad (6)$$

where the potential's parameters were [16]: D_W=0.9906eV, B_W=14.116nm^{-1}, R_W=0.3032nm.

To describe the interaction between an argon and tungsten atom, we applied the Lennard-Jones potential function:

$$\Phi_{W-Ar} = \begin{cases} 4\varepsilon_{WAr} \left[\left(\frac{R_{WAr}}{r} \right)^{12} - \left(\frac{R_{WAr}}{r} \right)^{6} \right], 0 < r < 2.5R_{WAr} \\ 0, r \geq 2.5R_{WAr} \end{cases}, \quad (7)$$

where the parameter values used were: ε_{WAr}/k_B=25.17K, R_{WAr}=2.93Å.

The Lennard-Jones 6-12 potential was also used to describe argon-argon interactions, with the parameter ε_{Ar}/k_B=119.18K. The adequacy of the chosen model for the interaction of argon atoms with tungsten discussed in detail in our previous work [14].

The second order velocity Verlet scheme [15, 16] with time step of Δt=10^{-16}s (smaller than the characteristic time of atom interactions) was used for an integration of equations of motion. The computational process was continued until all the net flux between the tanks does not become stable.

It should be noted that MD simulations are very time consuming, on the other hand, processes related to rarefied gas flow are characterized by long time of after which the flow becomes steady. The recent achievements in computer science allowed one to use the power of Graphic Processing Units (GPU) for computations. All simulations were performed using program code, developed by the authors of current work, on CUDA capable GPU. This parallel computation method allowed us to perform a vast number of simulations of systems involving up to several hundred thousand atoms. The detailed description of parallel program used for the current studies can be found in our previous work [17].

Results and discussions

At the first step we have compared our results with data published earlier by other researchers. Figure 3 represents correlation between dimensionless flow rate W versus channel's length-to-height ratio. The two limiting cases: and L_{ch}/h_{ch}>>1 are discussed in [18] and [13], respectively. In case of orifice (L_{ch}/h_{ch}=0) we have obtained W=0.538, while Sharipov and Kozak [18] reported W=0.539, the inequality is less than 1%. The derivation of analytical expression which allows calculating a mass flow through long channel of rectangular cross section is presented in [13]; this equation was derived with assumption of diffusive scatter of gas atoms on the channel's walls. In case of long channel (L_{ch}/h_{ch}>10) our results (crosses on Fig 3) coincide with predictions by analytical expression (diamonds on Fig 3) shown in [13]. These two issues allow us to conclude that current model gives physically adequate results and can be used for the further studies.

Correct choice of BC is one of the most important issues of simulations of rarified gas flow. According with theoretical results presented in [6] the flow rate decreases with respect to the accommodation coefficient on the channel's walls. Results of our previous study [14] show that argon – tungsten interactions are more specular than diffusive, especially in case of high temperature of the gas. This statement is also supported by results shown in Table 1.

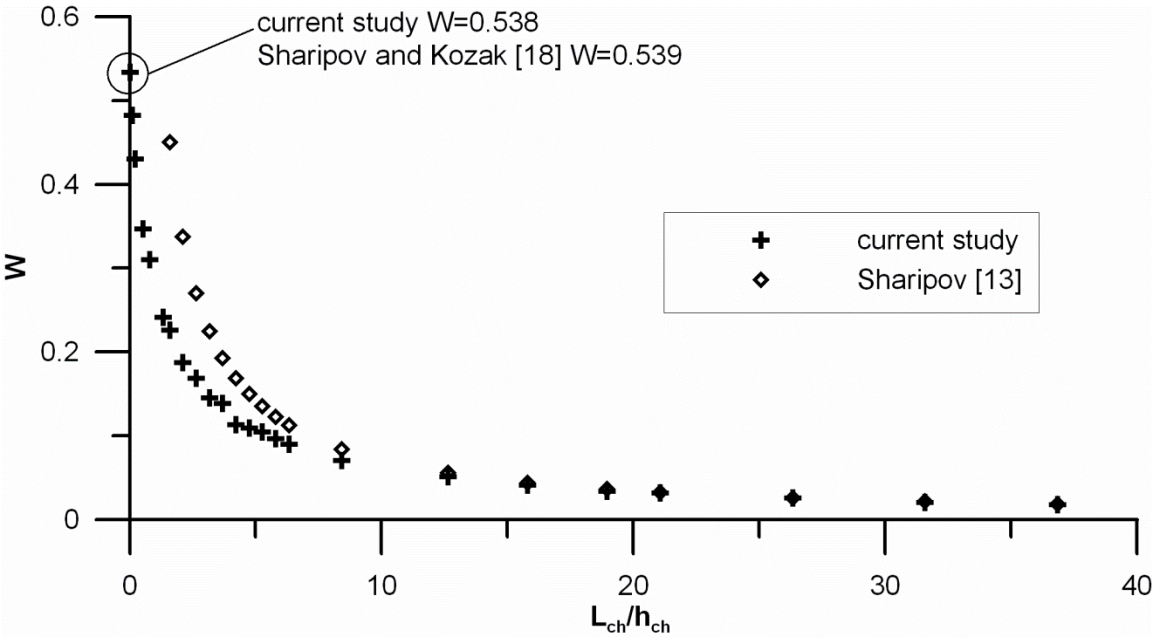

Figure 3. Normalized flow rate versus channel's length-to- height ratio. Parameters of simulations: $P_2/P_1 = 0.5$; $\delta = 0.2$, diffusive BC.

Table 1. Flow rate through the channel versus length to height ratio. W_{real} – flow rate through the real channel with smooth walls; W_{diff} – flow rate through the channels with diffusive BC.

L_{ch}/h_{ch}	W_{real}	W_{diff}	ε, %
0.55	0.388	0.343	13.3
1.08	0.309	0.265	16.6
2.68	0.206	0.170	20.9
4.80	0.144	0.116	24.1

The last column of Table 1 represents that the flow through the real channel with smooth walls is greater than the flow through the channel with diffusive BC, and this superiority increases with respect to the channel's length. The observed discrepancy is due to the probability of positive value of the dot product:

$$V^{is} = \overrightarrow{V^i} \cdot \overrightarrow{V^s}, \tag{8}$$

where V^i is the velocity of gas atom before collision with the surface; V^s is the velocity of gas atom before scattered by the surface.

In case of diffuse BC the probability of having positive value of Vis is 50%, while in case of the smooth tungsten surface this probability depends on atom's parameters of incidence and usually is greater than 50%. This statement is in accord with results of Chase et al. [19].

Data shown in Figure 4 represent correlations between flow rate and pressure difference for a various types of boundary conditions. Grey circles correspond to results obtained experimentally by Sreekanth [9] and approximated using equation (1). One can see that first order polynomial can fir the data points perfectly, while the slope of the approximation line is so-called hydrodynamics conductance. Table 2 represents values of hydrodynamics conductance of the channels with various BC as well as it gives explanations about the types of real channels mentions in Figure 4.

It is obvious that channel with specular BC has maximum conductance, because the dot product (8) has negative value only if the atom falls on the mirror-like surface normally. Parameters A and B correspond to the amplitude and wavelength of the roughness on the channel's walls, respec-

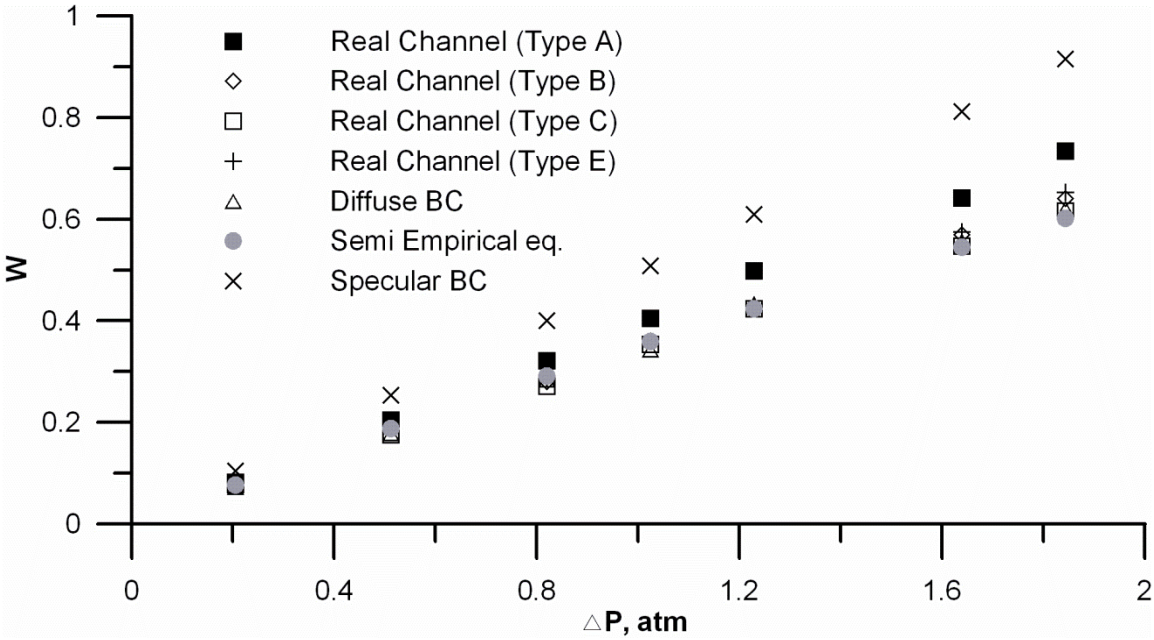

Figure 4. Normalized flow rate versus pressure difference.

Table 2. Hydrodynamic conductance of the channel with various boundary conditions on the walls. Parameters *A* and *B* are the amplitude and wavelength of the roughness on the walls, respectively.

	A, 10^{-10}m	B, 10^{-10}m	C_{hyd}, atm^{-1}
Real Channel (Type A)	0	-	0.3969
Real Channel (Type B)	3.16	6.32	0.3485
Real Channel (Type C)	1.58	6.32	0.3376
Real Channel (Type E)	1.58	12.64	0.352
Diffuse BC			0.341
Semi Empirical eq. by Sreekanth [9]			0.3372
Specular BC			0.4955

tively. One can see that channel with smooth walls (Type A) has lower hydrodynamic resistance than any other one considered in this study (except the case with specular BC). On the other hand diffuse BCs give result that has good agreement with experimental study, but it should be noted that the result corresponding to the case of rough channel of Type C fits semi empirical relation almost perfect. The last statement means that the assumption of diffuse BC obstructs us to predict of behavior of rarefied flow through the channel produced with high level of precision.

Conclusion

Rarefied gas flow between two tanks has been considered in the study and our results are in a good agreement with theoretical and experimental studies of other researches. On the other hand, have found that diffuse boundary conditions represent rough wall rather than the smooth one. The discrepancy of 15% between the value of hydrodynamic conductance measured in simulations of gas flow through the smooth tungsten channel and the conductivity obtained from semi empirical equation has been observed. We can conclude that flows inside the channel produced with high level of precision cannot be modeled using assumption of diffuse BC and the more complex model of BC is required.

Acknowledgments

The authors would like to acknowledge the kind funding support from NSC Taiwan under the contracts of NSC 101-2923-E-006-001-MY3.

REFERENCES

1. **Warrick, D. L., & Mack, E.** (1933). A Copper Membrane Gas-Molecule Sieve. Callendar's Theory of Osmosis. Journal of the American Chemical Society, 55(4), 1324-1332.
2. **Hanks, R. W., & Weissberg, H. L.** (1964). Slow Viscous Flow of Rarefied Gases through Short Tubes. Journal of Applied Physics, 35(1), 142-144.
3. **Shinagawa, H., Setyawan, H., Asai, T., Sugiyama, Y., & Okuyama, K.** (2002). An experimental and theoretical investigation of rarefied gas flow through circular tube of finite length. Chemical Engineering Science, 57(19), 4027-4036.
4. **Graur, I., & Sharipov, F.** (2009). Non-isothermal flow of rarefied gas through a long pipe with elliptic cross section. Microfluidics and Nanofluidics, 6(2), 267-275.
5. **Shen, C., Fan, J., & Xie, C.** (2003). Statistical simulation of rarefied gas flows in micro-channels. Journal of Computational Physics, 189(2), 512-526.
6. **Sharipov, F.** (1996). Rarefied gas flow through a long tube at any temperature ratio. Journal of Vacuum Science & Technology A: Vacuum, Surfaces, and Films, 14(4), 2627-2635.
7. **Lilly, T. C., Gimelshein, S. F., Ketsdever, A. D., & Markelov, G. N.** (2006). Measurements and computations of mass flow and momentum flux through short tubes in rarefied gases. Physics of Fluids, 18(9), 093601-093611.
8. **Fujimoto, T., & Usami, M.** (1984). Rarefied Gas Flow Through a Circular Orifice and Short Tubes. Journal of Fluids Engineering, 106(4), 367-373.
9. **Sreekanth, A.** (1965). Transition Flow through Short Circular Tubes. [10.1063/1.1761142]. Phys. Fluids, 8(11), 1951.
10. **Bernardo, P., Drioli, E., & Golemme, G.** (2009). Membrane Gas Separation: A Review/State of the Art. Industrial & Engineering Chemistry Research, 48(10), 4638-4663.
11. **Lu, J., & Lu, W.-Q.** (2010). A numerical simulation for mass transfer through the porous membrane of parallel straight channels. International Journal of Heat and Mass Transfer, 53(11–12), 2404-2413.
12. **Sharipov, F. M., & Seleznev, V. D.** (1994). Rarefied gas flow through a long tube at any pressure ratio. Journal of Vacuum Science & Technology A: Vacuum, Surfaces, and Films, 12(5), 2933-2935.
13. **Sharipov, F.** (1999). Rarefied gas flow through a long rectangular channel. Journal of Vacuum Science & Technology A: Vacuum, Surfaces, and Films, 17(5), 3062-3066.
14. **Leu, T.-S., Cheng, C.-H., & Ozhgibesov, M. S.** (2011). New modeling of scattering behaviors of argon atoms on tungsten substrate. Journal of Molecular Graphics and Modelling, 31(0), 35-40.
15. **Bird, G. A.** (1994). Molecular gas dynamics and the direct simulation of gas flows. Oxford New York: Clarendon Press ; Oxford University Press.
16. **S. Maruyama**, Molecular Dynamics Method for Microscale Heat Transfer. Advances in Numerical Heat Transfer, 2 (2000), pp. 189-226.
17. **Ozhgibesov, M.S., Utkin, A.V., Fomin, F.M., Leu, T.S., Cheng, C.H.** (2012). Simulation of cold copper deposition on the contaminated surface using gaming GPU. International Journal of Computational Materials Science and Engineering, in press
18. **Sharipov, F., & Kozak, D. V.** (2011). Rarefied gas flow through a thin slit at an arbitrary pressure ratio. European Journal of Mechanics - B/Fluids, 30(5), 543-549.
19. **Chase, D., Manning, M., Morgan, J. A., Nathanson, G. M., & Gerber, R. B.** (2000). Argon scattering from liquid indium: Simulations with embedded atom potentials and experiment. The Journal of Chemical Physics, 113(20), 9279-9287.